IARJSET

ISSN (Online) 2393-8021
ISSN (Print) 2394-1588

International Advanced Research Journal in Science, Engineering and Technology

Factura '20 - National Conference On Emerging Trends In Manufacturing

NSS College of Engineering, Palakkad, Kerala, India

Vol. 7, Special Issue 1, August 2020

Numerical Simulation of Friction Stir Welded Dissimilar Aluminium Alloys (AA6061-T6 and AA5086-O)

Muhammed Rashid P M[1], Arunkumar M[2]

M. Tech Student, Department of Mechanical Engineering, NSS College of Engineering, Palakkad, Kerala, India[1]

Assistant Professor, Department of Mechanical Engineering, NSS College of Engineering, Palakkad, Kerala, India [2]

Abstract: Friction Stir Welding is an advanced solid-state joining process invented as an alternative to joining materials that are unfavorable to be joined using a fusion welding technique. The non-consumable instrument is rotated in Friction Stir Welding and is slowly dipped into the middle line and moved along that line simultaneously. In the phase heat generation is a combined effect of frictional heating and heat due to material plastization. In this paper a thermo-mechanical model with enhanced potential is developed to research the temperature distribution, heat flux at the welding section and residual stress field formation in dissimilar materials. The average temperature obtained from the study is 4700C of aluminum alloys AA6061 to AA5086 are expected on model. Commercial finite element software ANSYS APDL® 19.2 is used for the friction stir welding simulation.

Keywords: Thermo-mechanical model, Heat flux, Residual stress and ANSYS APDL® 19.2.

I. INTRODUCTION

Friction Stir Welding (FSW) was invented at The Welding Institute (TWI) in the UK in 1991 as a solid-state joining technique and was initially applied to aluminium alloys. The basic concept of FSW is remarkably simple. A non-consumable rotating tool with a specially designed pin and shoulder is inserted into the abutment edges of the sheets or plates to be joined and crossed along the lines of the joint Figure. 1. The tool has two primary functions: (a) the heating of the work piece, and (b) the movement of the material to produce the joint. Heating is achieved by friction between the tool and the work piece and by plastic deformation of the work piece. The heating located around the pin softens the material and the combination of instrument rotation and translation results in movement of the material from the front of the pin to the rear of the pin. A joint is formed in "solid state" as a result of this process. The material flow around the pin can be very complicated because of different geometric characteristics.

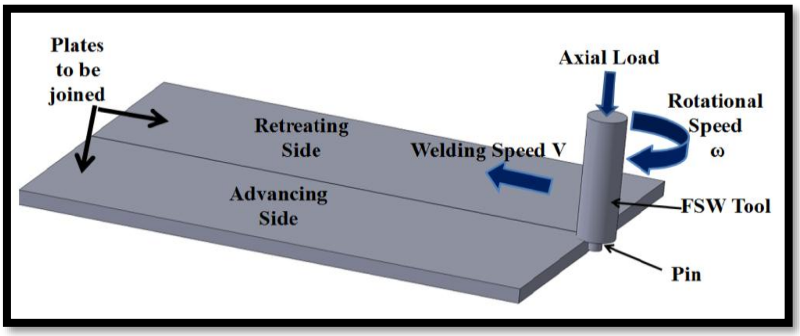

Figure1.Schematic diagram of FSW [3]

During the FSW process, the material is intensely plastically deformed and produces fine, equipped recrystallised grains at elevated temperatures. The thin microstructure provides strong mechanical properties in friction-stir solders. The work piece is positioned on a rear panel and tightened during the friction stir processing in a way that prevents the contiguous joints from pushing to separate. The FSW method consists of different phases; the tool, with a specially shaped projecting pin and a wider concentric shoulder, is gradually plunged into the joint line between two pieces of sheet or plate materials which are joined together until the shoulder rests on the surface: this is the plunging phase as shown in Figure (2(a)). The pin will have a one third diameter of the cylindrical tool and is usually slightly less long than the work piece size. At this point the friction coefficient in comparison with other processes is very high. In fact, the pin requires more torque and plunging power. The motion of the sink ends after the shoulder reaches the work surface and the phase of residence begins as shown in Figure (2(b)). The tool rotates without plunging in the work piece during this process. Between the wear-proof welding tool and the work piece material, frictional heat is produced. This heat softens the work pieces without approaching the point of melting. The coefficient of friction

IARJSET
ISSN (Online) 2393-8021
ISSN (Print) 2394-1588
International Advanced Research Journal in Science, Engineering and Technology
Factura '20 - National Conference On Emerging Trends In Manufacturing
NSS College of Engineering, Palakkad, Kerala, India
Vol. 7, Special Issue 1, August 2020

increases as the work piece softens. During this phase the heat generated is greater than the heat generated when the tool is moved. The rotating shoulder and pin deformation create a large palatized metal coating under and around the tool handle. When the shoulder comes together with new stuff, the plunging force increases. Energy continues to accumulate around the shoulder before this period of saturation occurs, as shown in Figure (2(c)). As the tool moves along the joint line, the plasticised material on the shear side is shattered to a flow side through a mechanical stirring and forging effect as shown in Figure (2(d)). The tool can be pushed along the joint line. This welding process gives the matted parts a good, completely integrated welding.

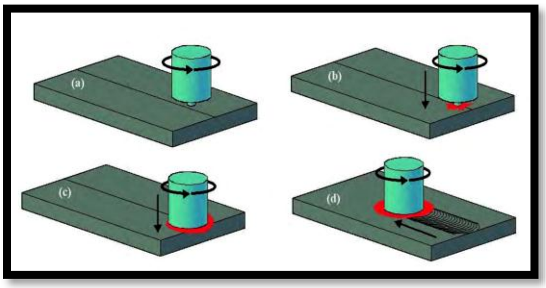

Fig2. FSW process steps [16]

II. NUMERICAL MODELLING

Calculations are based on discrete representations of particular welds with finite elements, finite differences or finite volume techniques. These methods can capture much of the complexity of material component behaviour, boundary conditions, and geometry, but the computational penalty means that a limited range of conditions tends to be studied in depth. Important stages in process modeling are:

i. Analytical Estimates of Heat Generation
ii. Heat Conduction
iii. Microstructure and Property Evolution in FSW
iv. Residual Stress

ANSYS 19.2 R, Commercial software is used to address transient friction stir lap joint thermal simulation. For solution the solver uses the following governing equations. The equation for heat conduction in 3D is:

$$\frac{\partial(\rho c T)}{\partial t} = \left[\frac{\partial}{\partial x}\left(k_x \frac{\partial T}{\partial x}\right) + \frac{\partial}{\partial y}\left(k_y \frac{\partial T}{\partial y}\right) + \frac{\partial}{\partial z}\left(k_z \frac{\partial T}{\partial z}\right) + Q\right]$$

Where,

K_x, K_y, K_z: Thermal conductivity in x,y,z directions (in this work all are equal)
ρ: density of work piece
Q: heat generated
x,y,z : three directions

The term Q is the plastic heat generated by friction at the interface between the tool and the work object. Generally, it's a volumetric phenomenon. Nonetheless, the heat generation by friction and plastic dispersion in most thermal models as in the current work, is modeled on a tool / work element interface as a surface heat flux. Modeling plastic waste as a volumetric heat source requires extensive information on the rate of plastic pressure and the stress of deviation. Thus it is necessary to develop a CFD model. Current research is to build a mechanical model for thermal energy.

The term Q is the plastic heat generated by friction at the interface between the tool and the work object. Generally, it's a volumetric phenomenon. Nonetheless, the heat generation by friction and plastic dispersion in most thermal models as in the current work, is modeled on a tool / work element interface as a surface heat flux. Modeling plastic waste as a volumetric heat source requires extensive information on the rate of plastic pressure and the stress of deviation.

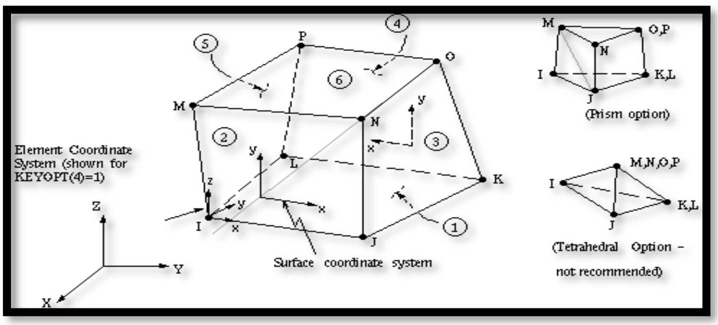

Fig 3.SOLID 186 element

IARJSET
ISSN (Online) 2393-8021
ISSN (Print) 2394-1588
International Advanced Research Journal in Science, Engineering and Technology
Factura '20 - National Conference On Emerging Trends In Manufacturing
NSS College of Engineering, Palakkad, Kerala, India
Vol. 7, Special Issue 1, August 2020

Thus it is necessary to develop a CFD model. Current research is to build a mechanical model for thermal energy. For transient thermal analysis SOLID 90 elements are used from the thermal mass method. 3D thermal conduction is assisted by this feature. Once the transient thermal analysis has been carried out, the thermal results are sequentially coupled at every phase of the time to overcome the thermo-elasticity.The defining the contacts between the work piece and tool are CONTA174 and TARGE170 are used in this analysis.

A moving source on the boundary of the weld line is put in the system's heat flow. This heat generated by contact between the frictional pin and the work piece is locally localized and rapidly propagates through the line of the plates, as well as by convection and radiation. Depending on the following equation, the total heat input can be determined.

Total Heat Input:

$$Q = \pi N \mu F \frac{R_o^2 + R_o * R_i + R_i^2}{45(R_o + R_i)}$$

Where,

Q = Total heat generated due to friction and plastic heat (Watts)
N = Rotation of tool (RPM)
μ = Coefficient of friction
F = Plunge force in the vertically downward direction (N)
R_o = Shoulder radius (m)
R_i = Pin radius (m)

It is assumed that the heat flux, q(r), is linearly distributed in the radial direction of the pin tool shoulder, and has the following form:

Heat flux:

$$q(r) = \frac{3Qr}{2\pi R_o^3}$$

Where $r \leq R_o$

The heat generated at the pin of tool is neglected because this heat is very small, e.g. in the order 2% of the total heat as reported by Russell and Shercliff. As such, the R_i is neglected in the equation. To summarize the heat generation utilized; the heat input is assumed to be linearly proportional to the distance from the center of the tool which is derived from the assumptions:The downward force applied to the work piece from the tool creates a uniform pressure between the shoulder and the work piece. The heat is generated from the work done by the friction force.

The friction coefficient is expected to decrease as the temperature increases and plastic forming function increases. The constant friction coefficient value of both thermal and synthetic factors during FSW is used in this model to estimate the complete effect. In order to be simpler, a uniform heat distribution across the surface of the shoulder is assumed for the heater generation in the vicinity of the pin as at the shoulder periphery, but the radius of the pin is equal. Therefore, the average radius of the shoulder and tool pin has been used for uniform distribution, i.e.

$$r = \frac{\text{Ro} + \text{Ri}}{2}$$

III. EXPERIMENTAL PROCEDURES

The experiment consists of welding of two dissimilar aluminum alloy (AA6061 and AA5086) joining with a H13 tool steel by friction stir welding. The work piece having the dimension 100*50*6 mm plates and having tool with tapered shape of a shoulder diameter 15mm and probe or pin diameter with a 5mm and pin length of 4.5 mm as shown in figure is used. A tool rotation speed of 840 RPM and a welding speed of 15 mm/min were used.

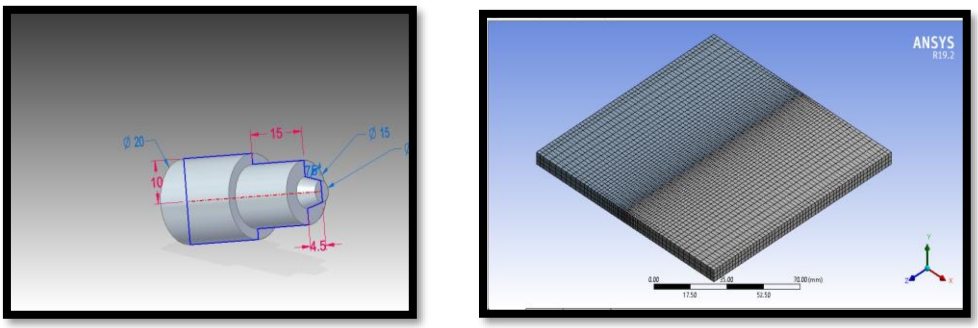

Fig 4. Schematic view of tool geometry and work piece geometry

IARJSET
ISSN (Online) 2393-8021
ISSN (Print) 2394-1588
International Advanced Research Journal in Science, Engineering and Technology
Factura '20 - National Conference On Emerging Trends In Manufacturing
NSS College of Engineering, Palakkad, Kerala, India
Vol. 7, Special Issue 1, August 2020

A. Simulation in Ansys

The simulation is done with the ANSYS APDL R19.2 has to be done with both thermal (transient) and structural analysis. The major step involved in the simulation as below.

- Three dimensional preparations for solid model in ANSYS as per work piece dimension.
- The material's temperature-dependent property as defined in the table was applied.
- The elements were selected to SOLID90 in ANSYS.
- Use the element of the tetra to mesh the components
- Full heat stream applied as a boundary condition on the surface of the product.
- Apply the air / work piece heat convection as 20W / m^2K
- Apply 1000W / m^2 K heat convection at the bottom of the plate.
- Time was measured and applied in the sub phase time according to the welding rate.
- Results viewed, graphs with time and displacement required for the variable required, contour diagrams, etc.

The thermal analysis temperature histories are implemented in the mechanical research as body loads. The only forces considered in this analysis are the strengths of the thermal expansion of the work piece material. For mechanical analysis, the following boundary conditions are used:

- Vertical motion at the lower surface of the work piece is constrained.
- A pin area is fastened to the work piece.
- No symmetric surface displacements.

IV. RESULTS AND DISCUSSIONS

A.Temperature Distribution

Heat is generated during the metal deformation by a combination of friction and plastic dissipation. Determination of heat production mechanisms depends on the soldering parameters, thermal conductivity of the portion of the work piece, the pin tool and anvil support and soldering geometry. Both the pin and the shoulder's weld geometrical characteristics influence how both surfaces slip, join, or alternate. When AA 5086-O on the forward side and AA 6061-T6 on the withdrawing side at different times, the temperature profile is obtained. AA6061 is heat affected region above AA5086 because heat transfer to AA6061 is higher. Due to its greater thermal diffusiveness, the majority of the heat generated at the interface is transferred to AA 6061. Figures show the variation of temperature for a friction time. The peak temperature obtained from the simulation at 5sec, 10sec, 15sec, 20sec and 24sec are 471 ^{0}C,467.09 ^{0}C, 471.89^{0}C, 465.5 ^{0}C and 467.22 ^{0}C are respectively as shown in figures below fig.5 which is significantly less than the melting temperatures of work-pieces and is within accepted temperature range in FSW process. The maximum temperature obtained is close to the weld centre line in the AA5086 side because it has a higher solidus temperature.

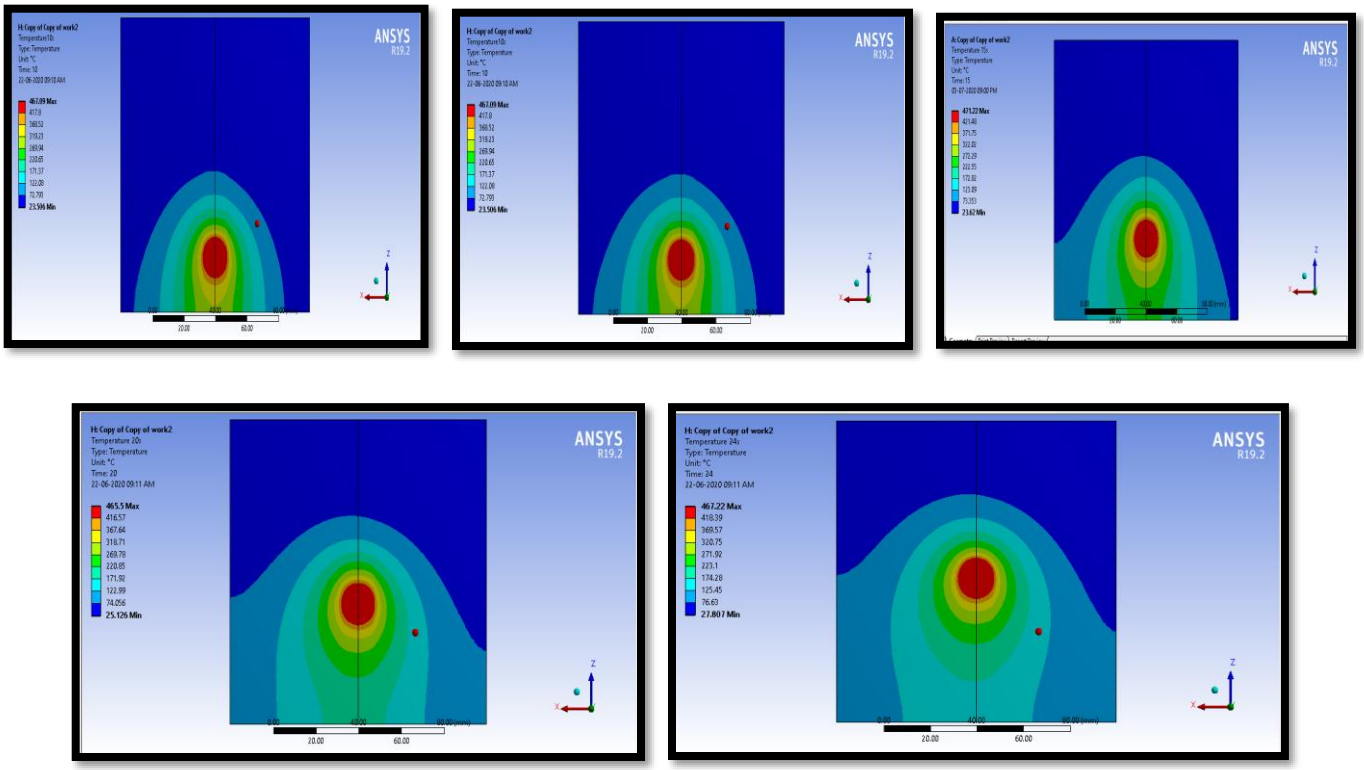

Fig 5. Temperature distributions at different times

ISSN (Online) 2393-8021
ISSN (Print) 2394-1588

International Advanced Research Journal in Science, Engineering and Technology

Factura '20 - National Conference On Emerging Trends In Manufacturing

NSS College of Engineering, Palakkad, Kerala, India

Vol. 7, Special Issue 1, August 2020

B. Thermal Flux

A single working component model is standardized in type of distributed heat source. The current intensity flux transformed into thermal energy gives the thermal source for the work piece in the present work. The thermal flux measured from the current input differs in heat delivery to parts of the device. Thermal flux findings are shown in the work pieces in the figures 6 along z(a), x(b) and y(c) axes. Various colors (or shades) show different thermal flow values.

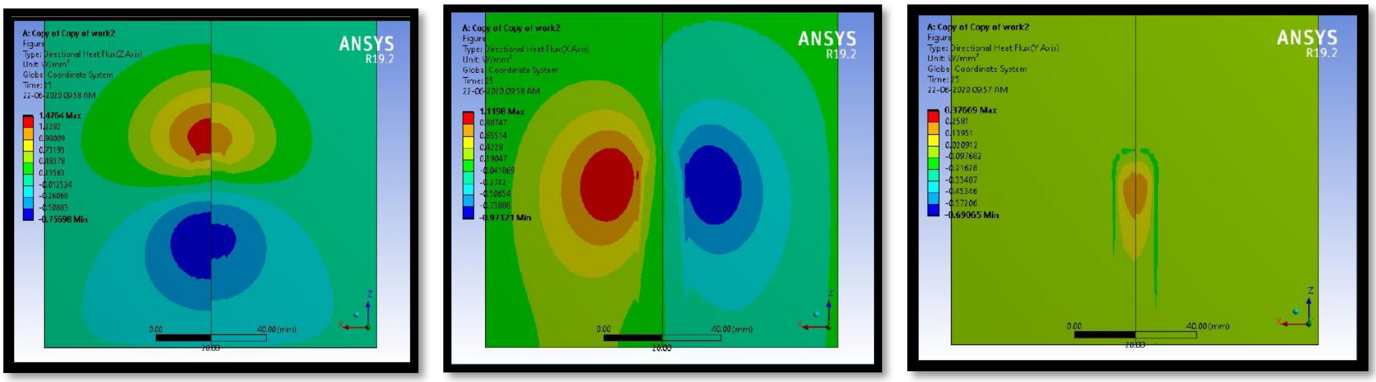

Fig6.Directional heat flux along z(a), x(b) and y(c) axes

The total heat flux produced at various temperatures and times is shown in the figures. The heat flux increases as well as the temperature and time. The average 24sect heat flow and a heat flow rate of 18.45W / mm^2 are shown in the figures 7 below, showing the total heat flow at different time

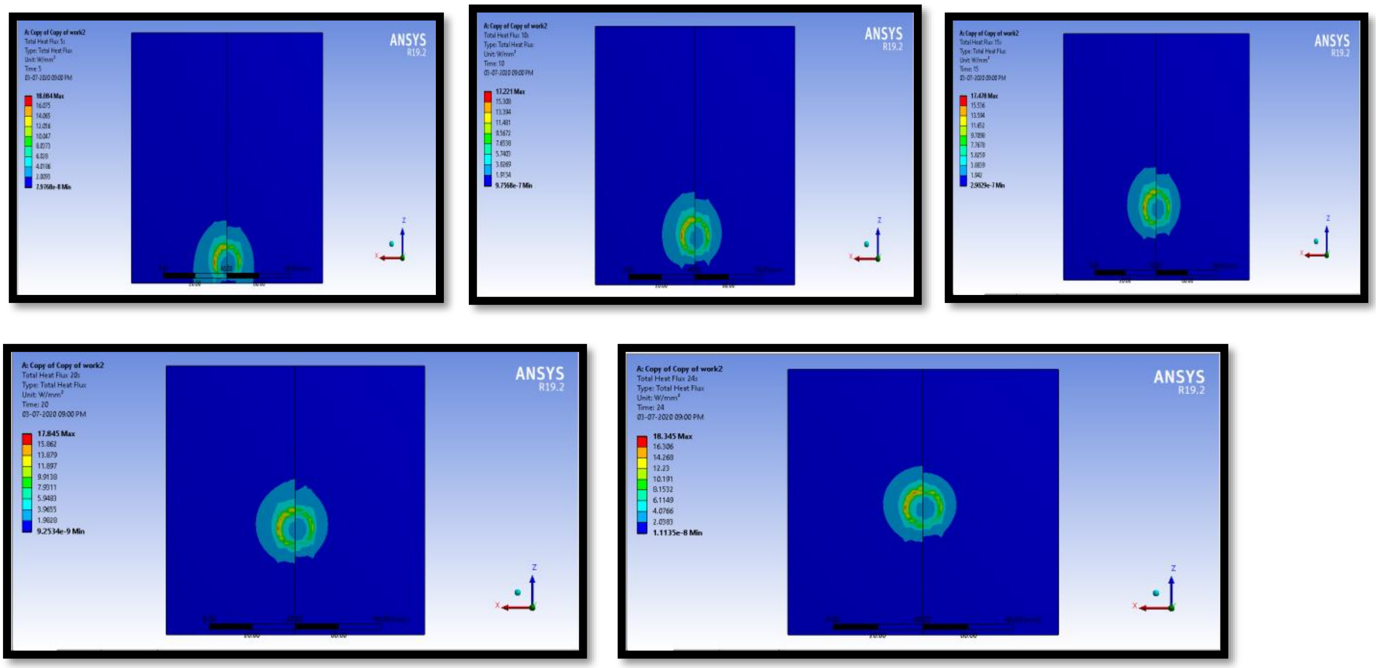

Fig 7. Total heat flux at different time

C. Stress Responses

The pressures are generated in the solder during the welding, and during heating of the soldered plates the material expands and afterwards, the welds are cooled down. In addition, because of the mechanical constraints of the plates through the fixture, the rotational and transverse motions of the tool cause additional stress to the weld. During the FSW process, significant residual pressure is frequently generated and the structural integrity and performance of components are deteriorated considerably. Within the FSW joints there are both tensile and compressive residual stresses. There are maximum residual stresses in the HAZ and minimal residual compressive pressure is found on the forward side just outside the soldering line. For the mechanical simulation for the calculation of waste stresses, the temperature fields generated by the thermal model are used. The estimated longitudinal and cross-stress distributions are shown in Figure 8. The longeritudinal stresses along the solder centre line can be seen to be compressive, with its nature changing gradually to tensile outside the heat-impacted zone and with the welds, due to mechanical constraints, as well to the high thermal stress generated during long welding times, the longitudinal stresses are progressively increased. The maximum tensile longitudinal stress obtained is approximately 776.24MPa, while 605.55MPa is observed also for the maximum transverse stress. The projections show that the maximum longitudinal stress is bigger in comparison with the maximal transverse stress, and longitudinal compressive stresses are also spread around the pin while longitudinal stress is mainly caused in areas far from the weld line at the edge of the sample. As anticipated because of the geometry of the plate, direction of welding and mechanical boundary conditions, length stresses are very small compared with transverse stresses.

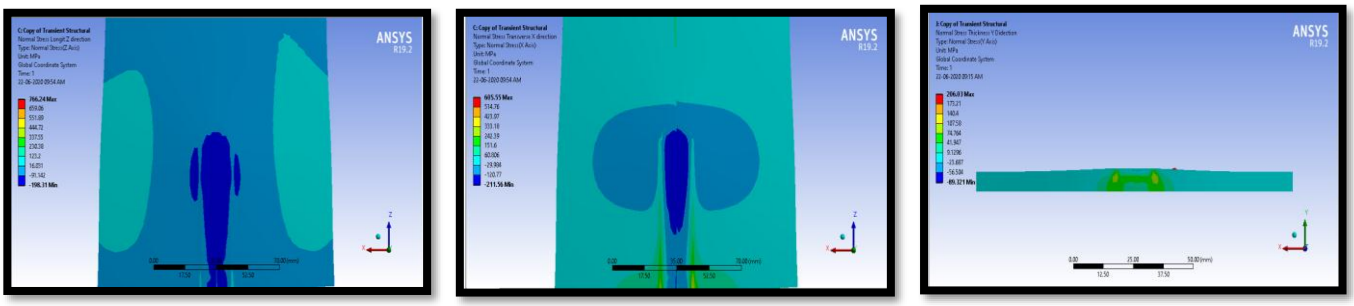

Fig 8. Stress distribution along different directions.

V. CONCLUSION

1. The thermal and structural effects simulated with ANSYS ® 19.2 are used for the assessment of temperature distribution and residual stress in the structure of the work piece.
2. Three-dimensional analysis models that are reliable and efficient for FSW welding simulation are developed using ANSYS.
3. The effect also increases the heat flow to a certain degree as the temperature increases.
4. The theoretical value i.e. under the melting point of the work is agreed on the temperature obtained by the simulation.
5. The longitudinal residual stresses are about 20-30% transverse of the residual stresses.

REFERENCES

[1] W.M. Thomas, E.D. Nicholas, J.C. Needham, M.G. Murch, P. Templesmith, C.J. Dawes, G.B. Patent Application No.9125978.8 (December 1991).
[2] C. Dawes, W. Thomas, TWI Bulletin 6, November/December 1995, p. 124.
[3] En-zhi GAO ,Xing-xing ZHANG, Chun-zhong, LIU,Zong-yi MA "Numerical simulation on material flow behaviors in whole process of friction stir welding" Transactions if Nonferrous Metals Society of china ,Vol 28,Iissue 11,2018,2324-2334.
[4] Caterina Casavola, Alberto Cazzato and Vincenzo Moramarco"Residual stress in friction stir welding and laser assisted friction stir welding by numerical simulation and experiments", 2017
[5] Prasanna, P., Rao, B.S. & Rao, G.K.M." Finite element modeling for maximum temperature in friction stir welding and its validation". Int J Adv Manuf Technol 51, 925–933 (2010). https://doi.org/10.1007/s00170-010-2693-4
[6] Varun Kumar A, M Balasrinivasan , R. Varun Kumar, K Balachandar, C Sivakumar"Temperature distribution study of Friction stir welded aluminum alloy 7075-T6 joints reinforced with SiC powders" ICMMM 2019, Materials Today: Proceedings 22 (2020) 1333–1340.
[7] Xiaocong He , Fengshou Gu , "Andrew Ball A review of numerical analysis of friction stir welding" Progress in Materials Science 65 (2014) 1–66.
[8]T.Pavan Kumar, Madhu Anupoju, Ramanjaneya Reddy Munnangi, Dr.Prabhakar Reddy "Friction Stir Welding (FSW) Simulation using FEA Techniques-Parametric Study using Ansys APDL"*IJSRD* || National Conference on Recent Trends & Innovations in Mechanical Engineering || April 2016, 2321-0613
[9]H.Jamshidi Aval, S. Serajzadeh∗, A.H. Kokabi "Evolution of microstructures and mechanical properties in similar and dissimilar friction stir welding of AA5086 and AA6061" Materials Science and Engineering A 528 (2011) 8071– 8083.
[10] Abhinand "Numerical Simulation of Friction Stir Welding for Dissimilar Metal Welding" AMMMT 2016, Materials Today: Proceedings 4(2017) 11265–11269
[11] A.F. Hasan "CFD modelling of friction stir welding (FSW) process of AZ31 magnesium alloy using volume of fluid method" journal of materials Research and Technology. 2019; 8(2):1819–1827
[12] Vinayak Malik, Sanjeev N K, H. Suresh Hebbarb, Satish V. Kailas "Investigations on the Effect of Various Tool Pin Profiles in Friction Stir Welding Using Finite Element Simulations" 12th GLOBAL CONGRESS ON MANUFACTURING AND MANAGEMENT, GCMM 2014 , Procedia Engineering 97 (2014) 1060 – 1068.
[13] Shuai Zhang, Gaoqiang Chen, Qu Liu, Han Li, Gong Zhang, Guoqing Wang, Qingyu Shi," Numerical analysis and analytical modeling of the spatial distribution of heat flux during friction stir welding" Journal of Manufacturing Processes 33 (2018) 245–255.
[14] The Welding Institute (TWI).
[15] ANSYS R19.2. Documentation.
[16] M.W. Mahoney and S.P. Lynch, "Friction Stir Processing"
[17] ASME, material composition chart of different aluminum alloys.

BIOGRAPHIES

Mr. Muhammed Rashid P, Completed M Tech mechanical engineering with specialization in computer integrated manufacturing from NSS College of Engineering, Palakkad, Kerala, India under APJ Abdul Kalam Technological University Kerala in the year 2020.

Mr. Arunkumar M